Visual Opsin Diversity in Sharks and Rays

Nathan S. Hart [ORCID],*,[1] Trevor D. Lamb,[2] Hardip R. Patel,[3] Aaron Chuah,[4] Riccardo C. Natoli,[2,5] Nicholas J. Hudson,[6] Scott C. Cutmore,[7] Wayne I.L. Davies,[8] Shaun P. Collin,[9] and David M. Hunt[10,11]

[1]Department of Biological Sciences, Macquarie University, North Ryde, NSW, Australia

[2]Eccles Institute of Neuroscience, John Curtin School of Medical Research, The Australian National University, Canberra, ACT, Australia

[3]Department of Genome Sciences, John Curtin School of Medical Research, The Australian National University, Canberra, ACT, Australia

[4]Department of Immunology and Infectious Disease, John Curtin School of Medical Research, The Australian National University, Canberra, ACT, Australia

[5]ANU Medical School, The Australian National University, Canberra, ACT, Australia

[6]School of Agriculture and Food Sciences, The University of Queensland, St Lucia, QLD, Australia

[7]School of Biological Sciences, The University of Queensland, St Lucia, QLD, Australia

[8]Umeå Centre for Molecular Medicine (UCMM), Umeå University, Umeå, Sweden

[9]School of Life Sciences, La Trobe University, Bundoora, VIC, Australia

[10]School of Biological Sciences, The University of Western Australia, Crawley, WA, Australia

[11]Centre for Ophthalmology and Visual Science, Lions Eye Institute, The University of Western Australia, Crawley, WA, Australia

*Corresponding author: E-mail: nathan.hart@mq.edu.au.

Associate editor: Belinda Chang

Abstract

The diversity of color vision systems found in extant vertebrates suggests that different evolutionary selection pressures have driven specializations in photoreceptor complement and visual pigment spectral tuning appropriate for an animal's behavior, habitat, and life history. Aquatic vertebrates in particular show high variability in chromatic vision and have become important models for understanding the role of color vision in prey detection, predator avoidance, and social interactions. In this study, we examined the capacity for chromatic vision in elasmobranch fishes, a group that have received relatively little attention to date. We used microspectrophotometry to measure the spectral absorbance of the visual pigments in the outer segments of individual photoreceptors from several ray and shark species, and we sequenced the opsin mRNAs obtained from the retinas of the same species, as well as from additional elasmobranch species. We reveal the phylogenetically widespread occurrence of dichromatic color vision in rays based on two cone opsins, RH2 and LWS. We also confirm that all shark species studied to date appear to be cone monochromats but report that in different species the single cone opsin may be of either the LWS or the RH2 class. From this, we infer that cone monochromacy in sharks has evolved independently on multiple occasions. Together with earlier discoveries in secondarily aquatic marine mammals, this suggests that cone-based color vision may be of little use for large marine predators, such as sharks, pinnipeds, and cetaceans.

Key words: opsin evolution, vertebrate vision, elasmobranchs, cone monochromacy, spectral tuning.

Introduction

With very few exceptions, color vision in vertebrates is made possible by the presence in the retina of two or more spectrally distinct classes of cone photoreceptor. The visual pigments expressed in cones are termed cone opsins and, on the basis of nucleotide and amino acid sequence homology, each is assigned to one of the following four classes: SWS1, SWS2, RH2, or LWS (these names derive from "short-wavelength-sensitive", "rhodopsin-like", and "long-wavelength-sensitive", respectively). Within each of the four classes of cone opsin, there is considerable variation in the position of the spectral absorbance peak (λ_{max}) across species. This is a result of "spectral tuning" mediated by the presence of different amino acid residues in the vicinity of the light-absorbing chromophore, which in most terrestrial vertebrates is 11-*cis* retinal (A_1). As a general guide, the λ_{max} values for A_1-based cone opsins (rhodopsins) typically fall in the ranges: SWS1 $\sim$360–440 nm; SWS2 $\sim$400–480 nm; RH2 $\sim$440–530 nm; and LWS $\sim$495–575 nm (Yokoyama 2008; Cortesi et al. 2015).

As well as the "visual opsins", comprising the above four cone opsins plus the rod opsin (RH1), the vertebrate genome encodes several other closely related C-opsins (ciliary opsins), so called because of their expression in ciliated photoreceptor cells. These related C-opsins include pinopsin, vertebrate ancient opsin, parietopsin, parapinopsin, encephalopsin (OPN3), and the teleost multiple tissue (TMT) opsins, many of which are expressed at low levels in the retina, and/or at higher levels in other structures that arise from
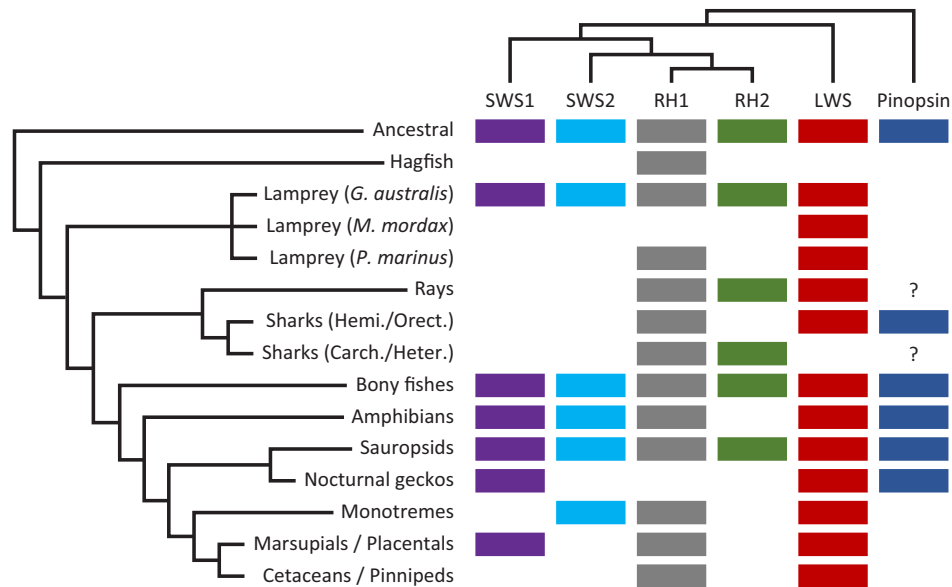
FIG. 1. Schematic diagram showing the retention and loss of visual opsin classes in selected taxa. Lines at left indicate species divergences; lines at top indicate gene duplications for opsin classes. Abbreviations for shark families: Hemi, Hemiscyllidae; Orect, Orectolobidae; Carch, Carcharhinidae; Heter, Heterodontidae.

the developing diencephalon, such as the pineal organ, the parapineal organ, or the parietal eye. On the other hand, the expression of OPN3 and some TMTs may occur primarily in nonocular structures, such as skin, heart, and liver (Peirson et al. 2009). These "nonvisual opsins" are generally thought to drive nonvisual light-dependent mechanisms, such as circadian rhythms, seasonal reproduction, and neural development. However, compared with teleost and holostean fishes (Beaudry et al. 2017), very little is known about the diversity and function of nonvisual C-opsins in cartilaginous fishes, and it has been suggested that pinopsin may play a role in vision in some vertebrates (Sato et al. 2018).

The vertebrate ancestor possessed rod opsin plus all four classes of cone opsin, and all five classes have been retained in many species of reptiles, birds, and fishes (Yokoyama 2000; Collin et al. 2003). But, as illustrated schematically in figure 1, various vertebrate lineages have lost some (or, in a few extreme cases, all) of the cone opsin gene classes. For example, placental mammals and marsupials have lost the SWS2 and RH2 opsin gene classes (Deeb et al. 2003; Jacobs 2009), whereas monotremes (egg-laying mammals) have lost the SWS1 and RH2 opsin gene classes (Davies, Carvalho, et al. 2007; Wakefield et al. 2008). In both cases, the loss is potentially attributable to a mesopic or nocturnal "bottleneck" during early mammalian evolution (Walls 1963; Davies et al. 2012). As a result, color vision in most mammals is dichromatic, being mediated by either the SWS1 or SWS2 cone opsin class combined with the LWS cone opsin class (Jacobs 2009).

Marine mammals, except for the sirenians (dugongs and their relatives), have additionally lost the SWS1 opsin gene class, to become cone monochromats with their photopic vision mediated by the LWS opsin, so that they have nonexistent (or minimal) color vision (Peichl 2005). It has been suggested that cone monochromacy in marine mammals

evolved because of the light environment in the habitats that they would have occupied during their transition from land into water (Peichl et al. 2001), that is, riverine and coastal waters that typically have high turbidity and a predominance of longer wavelengths due to high concentrations of dissolved organic matter and chlorophyll (Jerlov 1976). Interestingly, deep-diving whales appear to have subsequently lost all cone classes (Meredith et al. 2013), with a potential impact on their range of visual sensitivity.

In this study, we examine the less well-studied cases of cone dichromacy and cone monochromacy in elasmobranch fishes. Several species of ray have been shown to possess two cone pigments (Hart et al. 2004; Theiss et al. 2007; Bedore et al. 2013), with the likelihood that they are cone dichromats with functional color vision (Van-Eyk et al. 2011). Those few species of shark that have been studied to date have been found to possess just a single spectral class of cone (Hart et al. 2011), apparently containing the LWS opsin (Theiss et al. 2012), with the consequence that they are almost certainly cone monochromats and lack color vision (Schluessel et al. 2014). Here, we characterize the molecular identity of the retinal visual pigments expressed in five species of shark and four species of ray, focusing on shallow-dwelling species known or likely to possess cone photoreceptors, and those filling particular phylogenetic gaps. Furthermore, we provide measurements of the spectral characteristics of the visual pigments expressed in nine species of ray and two species of shark. We confirm that all the shark species studied to date appear to be cone monochromats but report that in different species the single cone opsin may be of either the LWS or the RH2 class. We then discuss the origins of di- and monochromacy in marine vertebrates and consider the selection pressures driving adaptation in elasmobranch visual pigments.

Table 1. Mean Wavelength of Maximum Absorbance (λ_{max}) Values for the Rod and Cone Visual Pigments of Selected Batoid Species Measured Using Microspectrophotometry.

Family/Common Name (binomial name)	λ_{max} (nm)			
	Rod (mature)	Rod (immature)	S-Cone	L-Cone
Dasyatidae				
Estuary ray (*Dasyatis fluviorum*)[1]	500.2±1.4 (31)		474.9±3.4 (24)	566.0±2.8 (29)
Pink whipray (*Himantura fai*)[1]	502.6±2.5 (20)		475.3±5.4 (13)	556.8±5.7 (17)
Bluespotted maskray (*Neotrygon kuhlii*)[2]	496.7±1.7 (37)	498.4 ± 3.6 (8)	475.9±4.2 (13)	552.1 ± 8.4 (11)
Bluespotted fantail ray (*Taeniura lymma*)[1]	500.0±1.5 (14)		479.4±3.5 (4)	557.2±3.9 (9)
Gymnuridae				
Australian butterfly ray (*Gymnura australis*)[1]	500.3±1.0 (33)		466.6±3.4 (21)	556.1±2.3 (33)
Myliobatidae				
Spotted eagle ray (*Aetobatus narinari*)[1]	502.0±1.1 (17)		450.4±6.6 (4)	551.7±3.0 (13)
Rhinobatidae				
Eastern shovelnose ray (*Aptychotrema rostrata*)[3]	498.1±1.9 (15)	491.8 ± 3.3 (5)	458.7±3.1 (10)	553.2±4.4 (11)
Western shovelnose ray (*Aptychotrema vincentiana*)[1]	499.8±1.3 (18)	500.7±3.5 (6)	460.3±3.4 (11)	557.3±5.4 (15)
Giant shovelnose ray (*Glaucostegus typus*)[3]	504.2±1.9 (14)	502.0±2.8 (5)	476.6±4.2 (10)	561.1±4.8 (10)
Eastern fiddler ray (*Trygonorrhina fasciata*)[1]	498.6±0.7 (20)		470.1±2.9 (15)	567.9±2.8 (23)
Atlantic guitarfish (*Rhinobatos lentiginosus*)[4]	~496	498.7±0.7 (9)		
Rhinopteridae				
Cownose ray (*Rhinoptera bonasus*)[5]	500±2 (28)		470±1 (6)	551±2 (16)
Rhynchobatidae				
White-spotted guitarfish (*Rhynchobatus australiae*)[1]	499.9±1.2 (21)		475.2±3.9 (20)	554.6±2.6 (25)
Urolophidae				
Common stingaree (*Trygonoptera testacea*)[1]	497.6±1.6 (13)		480.9±14.9 (2)	556.5±2.5 (5)
Urotrygonidae				
Yellow stingray (*Urobatis jamaicensis*)[5]	499±2 (23)		475±2 (6)	562±3 (32)
				533±4 (2)

NOTE.—Mean prebleach absorbance spectrum λ_{max} values are given ±1 SD. Number of cells used in the analysis are given in parentheses. Taxonomic classification follows that given by Eschmeyer et al. (2016). Data obtained from: [1]this study, [2]Theiss et al. (2007), [3]Hart et al. (2004), [4]Gruber et al. (1990), [5]Bedore et al. (2013).

Results

Microspectrophotometry of Elasmobranch Visual Pigments

The retinae of all species studied contain both rod and cone photoreceptors and are therefore "duplex" in anatomical terms. The dimensions of the outer segments examined are given in supplementary table S2, Supplementary Material online. The spectral parameters measured using microspectrophotometry from photoreceptor outer segments are collated in tables 1 and 2. Table 1 presents new measurements made in this study for nine species of ray, together with measurements from previous studies on another six species of ray for comparison. Table 2 presents measurements for ten species of shark, taken primarily from a previous study (Hart et al. 2011), but with new measurements from two additional species made in this study.

Figure 2 shows representative microspectrophotometric data for the rods and two cone classes measured in the butterfly ray, *Gymnura australis*. These mean absorbance spectra have been fitted with the A_1 visual pigment template proposed by Govardovskii et al. (2000), with individual λ_{max} values of 466 nm (S-cone), 500 nm (rod), and 556 nm (L-cone); in each case, the template provides an excellent fit to the data. For the nine species of ray studied here (table 1), the rod λ_{max} value (averaged across 13–33 cells in different species) was distributed over a narrow spectral range, from 497–504 nm. In these same species, there was a fairly broad distribution of mean λ_{max} values for the S-cones, from 450–481 nm, and an intermediate distribution of mean λ_{max} for

the L-cones from 552–568 nm. Based on the mRNA sequence data presented subsequently, we predict that the opsin gene expressed in each class of cell is as follows: rods, *RH1*; S-cones, *RH2*; L-cones, *LWS*.

For the two species of shark studied here, we were readily able to make MSP recordings from rods, but experienced considerable difficulties finding intact cone outer segments. As a result, we were able to obtain acceptable measurements from only two cone outer segments in the blacktip reef shark *Carcharhinus melanopterus*, but none in the gray reef shark *C. amblyrhynchos*. Figure 3 presents the mean absorbance spectra for the rod and cone visual pigments in *C. melanopterus*, with the cone spectrum exhibiting substantially more measurement noise due to the low number of spectra averaged. For the rods of these two species, we obtained mean λ_{max} values at 505 and 504 nm, and for the cones of *C. melanopterus* we obtained a mean λ_{max} at 528 nm (table 2). From the opsin sequences detected by transcriptome analysis, we predict that in this species the rods express the *RH1* opsin gene and the cones express the *RH2* opsin gene. Inspection of the cone pigment data in table 2, and the opsin sequence data in table 3, provides compelling evidence, firstly, that each of the shark species examined possesses just a single spectral class of cone and expresses only a single cone opsin and, secondly, that this cone opsin may be from either the LWS or the RH2 class. We shall consider the implications of these findings in the Discussion.

In one species of ray and one species of shark, we found several outer segments with a cone-like appearance, but with a pigment exhibiting a λ_{max} almost identical to that of the

Table 2. Mean Wavelength of Maximum Absorbance (λ_{max}) Values for the Rod and Cone Visual Pigments of Selected Shark Species Measured Using Microspectrophotometry.

Family/Common Name (binomial name)	λ_{max} (nm)			
	Rod (mature)	Rod (immature)	L-Cone	Cone Opsin Class
Carcharhinidae				
Pigeye shark (*Carcharhinus amboinensis*)[2]	507.4±5.2 (24)		534.1±8.9 (8)	?
Grey reef shark (*Carcharhinus amblyrhynchos*)[1]	503.6±2.2 (10)		NF	RH2
Bull shark (*Carcharhinus leucas*)[2a]	518.4±6.5 (47)		554.4±11.7 (45)	?
	(pred. A_1 = 509)		(pred. A_1 = 535)	
Common blacktip shark (*Carcharhinus limbatus*)[2]	505.6±1.8 (51)		531.8±3.9 (134)	RH2
Blacktip reef shark (*Carcharhinus melanopterus*)[1,2]	505.4±1.8 (30)	506.9±3.8 (9)	527.6±2.3 (2)	RH2
Dusky shark (*Carcharhinus obscurus*)[2]	502.4±2.1 (5)		NF	RH2
Australian sharpnose shark (*Rhizoprionodon taylori*)[2]	508.2±2.7 (18)		533.3±8.9 (6)	?
Hemiscyllidae				
Brown-banded bamboo shark (*Chiloscyllium punctatum*)[2]	499.6±2.6 (84)		531.8±6.7 (5)	LWS
Orectolobidae				
Spotted wobbegong (*Orectolobus maculatus*)[2]	484.4±3.9 (44)		552.8±4.8 (10)	LWS
Ornate wobbegong (*Orectolobus ornatus*)[2]	498.4±3.7 (45)		560.5±4.9 (10)	LWS

NOTE.—Mean prebleach absorbance spectrum λ_{max} values are given ±1 SD. Number of cells used in the analysis are given in parentheses. Taxonomic classification follows that given by Eschmeyer et al. (2016). Data obtained from: [1]this study, [2]Hart et al. (2011). NF, cone spectra not measured using MSP. The cone opsin class determined by sequence analysis of mRNA for the single cone opsin found in each species is shown, where relevant.
[a]Rod and cone visual pigments in the bull shark comprise a mixture of A_1 and A_2 chromophores and accordingly have longwave-shifted λ_{max} values; the predicted A_1 chromophore-only λ_{max} values are shown.
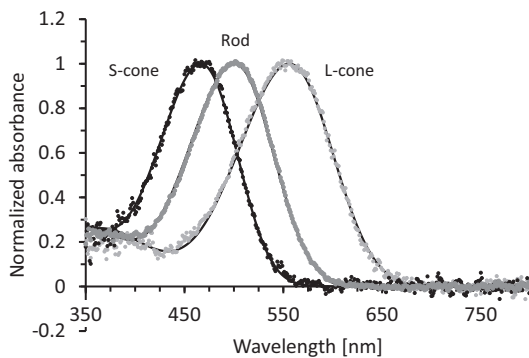

FIG. 2. Spectral absorbance of the rod and cone visual pigments in the retina of a representative ray species, the butterfly ray *Gymnura australis* measured using microspectrophotometry. S-cone, short-wavelength-sensitive cone; L-cone, long-wavelength-sensitive cone. Mean prebleach spectra (S-cones, $n = 21$; L-cones, $n = 33$; rods, $n = 33$) are shown fitted with the A_1 visual pigment template of Govardovskii et al. (2000) with λ_{max} values of 466, 500, and 556 nm.

rods present in the same species. For the western shovelnose ray *Aptychotrema vincentiana*, these cells had a mean λ_{max} at 501 nm, whereas the rods had a mean λ_{max} at 500 nm; for the blacktip reef shark *C. melanopterus*, these cells had a mean λ_{max} at 507 nm, whereas the rods had a mean λ_{max} at 505 nm (tables 1 and 2). In contrast to the more abundant S- and L-cones, the postbleach spectra of these cone-like cells displayed prominent absorbance peaks at approximately 380 and 480 nm, which are characteristic of the long-lived photoproducts (i.e., metarhodopsin II and III; Paulsen et al. 1975) seen in measurements of rods (supplementary fig. S1, Supplementary Material online). Furthermore, for both species, the animals we examined were juveniles. Accordingly, we hypothesize that these occasional cells were newly differentiated, immature *RH1*-expressing rods, with short and slightly
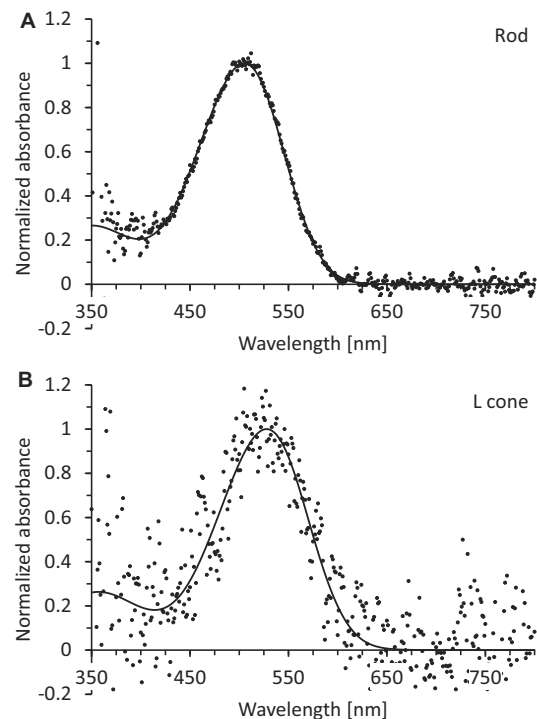

FIG. 3. Spectral absorbance of the rod (A) and cone (B) visual pigments in the retina of the black tip reef shark *Carcharhinus melanopterus* measured using microspectrophotometry. Mean prebleach spectra (rods, $n = 30$; L-cone, $n = 2$) are shown fitted with the A_1 visual pigment template of Govardovskii et al. (2000) with λ_{max} values of 505 (A) and 528 (B) nm.

tapering outer segments, as observed in the all-rod retinae of juvenile skates *Leucoraja* spp. (see figure 3 in Szamier and Ripps 1983). This would also explain the earlier finding of similar cone-like cells with a rod-like pigment in the giant shovelnose ray, eastern shovelnose ray, and bluespotted

Table 3. Amino Acid Residues at Key Spectral Tuning Sites and Spectral Absorbance Peaks for Elasmobranch Visual Opsins.

Opsin	Species	ID/Accession	83	118	122	164	181	189	207	211	261	265	269	292	295	308	λ_{max}(nm)	Ref.
RH1	Cattle	NP-001014890	D		E	A		I	M	H	F	W	A	A	A	M	499*	a
RH1	Giant shovelnose ray	CL599	D		E	A		V	M	H	F	W	A	A	A	L	504	b
RH1	Western shovelnose ray	46583-1-1	D		E	A		V	M	H	F	W	A	A	A	L	500	c
RH1	Bluespotted maskray	23396-1-1	D		E	A		V	M	H	F	W	A	A	A	L	497	d
RH1	Little skate	AAC60251	D		E	A		V	M	H	F	W	A	A	A	L	502	e
RH1	Bamboo shark	63210-1-1	D		E	A		I	M	H	F	W	A	A	A	L	500	f
RH1	Spotted wobbegong	AFS63881	D		E	A		I	M	H	F	W	A	S	A	L	484	f
RH1	Whale shark	XP-020378075	D		E	A		I	M	H	F	W	A	A	A	L	478*	g
RH1	Blackmouth catshark	CAA76798	N		E	A		I	M	H	F	W	A	S	A	L	482	h
RH1	Gray reef shark	63389-1-1	D		E	A		V	M	H	F	W	A	A	A	L	504	c
RH1	Blacktip reef shark	CL4386	D		E	A		V	M	H	F	W	A	A	A	L	505	c
RH1	Small spotted catshark	CAA76797	D		E	A		I	M	H	F	W	A	A	A	L	496	h
RH1	Velvet belly lanternshark	[See Ref. i]	N		E	A		V	M	H	F	W	A	A	A	L	488	i
RH1	Elephant shark	NP-001279181	D		E	A		V	M	H	F	W	A	A	A	L	496	j
RH2	Giant shovelnose ray	C418	N	T	Q	G		P	L	Y		W	A	A	S		477	b
RH2	Western shovelnose ray	31915-1-1	N	A	Q	G		P	L	H		W	A	A	S		460	c
RH2	Bluespotted maskray	30063-1-2	N	T	Q	G		P	L	Y		W	A	A	S		476	d
RH2	Gray reef shark	45084-1-2	G	T	E	A		P	L	H		W	A	A	A		?	
RH2	Blacktip reef shark	U16228	D	T	E	A		P	M	H		W	T	A	A		528	c
RH2	Common blacktip shark	CLI22-Partial	?	?	?	A		P	M	H		?	?	?	?		532	f
RH2	Dusky shark	NH26-37-Partial	?	?	?	A		P	M	H		W	T	A	A		?	
RH2	Elephant shark	NP-001279976	N	T	Q	A		P	L	H		W	A	S	S		442	j
RH2	Zebra bullhead shark	GGGL01052190	?	T	E	A		P	L	Y		W	A	A	S		?	
LWS	Cattle	NP-776991				A	H				Y		T	A			552*	k
LWS	Giant shovelnose ray	292w69				S	H				Y		T	A			561	b
LWS	Western shovelnose ray	28777-1-1				S	H				F		T	A			557	c
LWS	Bluespotted maskray	28822-1-1				S	H				F		T	A			552	d
LWS	Bamboo shark	16730-1-1				S	H				F		A	A			532	f
LWS	Spotted wobbegong	AFS63883				S	H				F		T	A			553	f
LWS	Elephant shark LWS1	NP-001304659				S	H				F		A	S			499	j
LWS	Elephant shark LWS2	NP-001279735				S	H				F		T	A			548	j
LWS	Whale shark	Rhity2000048				A	H				F		A	S			?	

NOTE.—Residues are given for putative key tuning sites referred to in the text for each opsin. Empty entries indicate that the sites are not of interest; "?" indicates unknown residue for partial sequences. Spectral peaks (λ_{max}) are from MSP measurements, except those marked "*", which were obtained using recombinant opsins. References are for λ_{max}: a, Fasick and Robinson (1998); b, Hart et al. (2004); c, this study; d, Theiss et al. (2007); e, Brin and Ripps (1977); f, Hart et al. (2011); g, Hara et al. (2018); h, Bozzano et al. (2001); i, Delroisse et al. (2018); j, Davies et al. (2008); k, Fasick et al. (2011).

maskray (Hart et al. 2004; Theiss et al. 2007), given that all of these rays have also now been shown to express only one rod opsin (RH1) and two cone opsin genes (RH2 and LWS) in the retina.

Molecular Phylogeny of Elasmobranch C-Opsins

Using both reverse-transcription polymerase chain reaction (RT-PCR) and whole-transcriptome sequencing approaches, we identified 43 C-opsin (ciliary opsin) mRNA sequences from shark and ray retinal tissue. Supplementary table S3, Supplementary Material online, lists these sequences, their GenBank accession numbers, and their transcript levels. The multiple sequence alignment for all the opsins that we analyzed is presented in supplementary file 1, Supplementary Material online. Figure 4 presents the molecular phylogeny that we obtained for a set of 202 vertebrate C-opsins (for cartilaginous and agnathan fishes as well as bony vertebrates). The tree is shown in collapsed form in figure 4 and in fully expanded form in supplementary figure S2, Supplementary Material online. For the analysis presented here, we chose not to include more distant C-opsins (such as OPN3, TMTs, or those from tunicates, lancelets, basal

deuterostomes, and protostomes), because their inclusion generated alignments that appeared less convincing. Nevertheless, we established that the root of this tree lies at the position of the arrow at the lower left, through preliminary analysis of a larger set of vertebrate opsins, including the melanopsins (OPN4s). In figure 4, the UFBoot2 bootstrap support level for every subtree and every node is at least 96%. Interestingly, this includes very high support for the position of pinopsin as sister to the five conventional opsins expressed in rods and cones, consistent with the notion that pinopsin could have diverged prior to the expansion of cone opsin isoforms and may play a role in scotopic vision in some vertebrates (Sato et al. 2018). The support levels estimated by UFBoot2 are typically higher than conventional bootstrap estimates, although there is evidence that they tend to be less biased (see Hoang et al. 2018 and Materials and Methods).

In figure 5, we have extracted those sections of supplementary figure S2, Supplementary Material online, that include cartilaginous fish species, where representatives were present from only five of the nine vertebrate opsin clades examined in
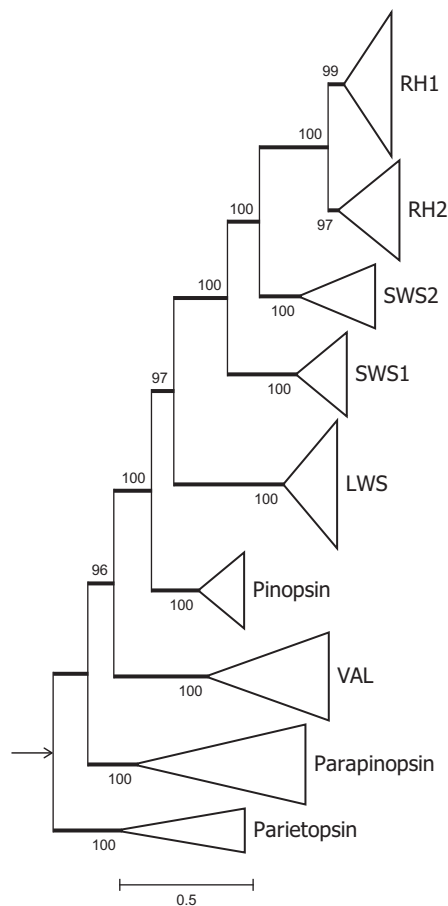
Fig. 4. Maximum likelihood (ML) molecular phylogeny for nine vertebrate C-opsin classes. The tree is shown collapsed, and the fully expanded tree is presented in supplementary figure S2, Supplementary Material online. A total of 202 vertebrate opsin protein sequences were aligned using MAFFT L-INS-i, and tree inference was performed using IQ Tree with the WAG protein substitution model (see Materials and Methods). The arrow indicates the presumed root. Scale bar denotes amino acid substitutions per site.

figure 4. The relative positions of taxa within these five subtrees conform fairly closely to the accepted species phylogeny (Vélez-Zuazo and Agnarsson 2011). The sequences denoted in bold font were obtained in the present study using retinal tissues, which suggests that the encoded proteins are expressed in the retina; the remaining sequences were obtained from the NCBI database and are not necessarily expressed in the retina. Thus, figure 5 provides evidence for retinal expression of RH1, RH2, LWS, and vertebrate ancient opsin (VAL) in rays; RH1 and RH2 in carcharhinid sharks; and RH1, LWS, and pinopsin in bamboo shark. Measurements of transcript levels (in units of RPKM-CDS, see supplementary table S3, Supplementary Material online) showed massive levels of RH1 ($>$10k) in each of these species, moderate levels of RH2 or LWS ($\sim$200, when present), but only trace levels of pinopsin and VAL ($<$10). The far higher transcript levels for the rod-based opsin (RH1) in comparison with the levels for the cone-based opsins (RH2 and LWS) reflect the fact that rods are more numerous and typically have larger outer segments than cones (Hart et al. 2006; Schieber et al. 2012).

We found no evidence, either in the present study or in databases, for the occurrence in cartilaginous fishes of any sequences from the following C-opsin clades: SWS1, SWS2, parietopsin, or TMT3. Furthermore, although the parapinopsin, OPN3, and TMT3 genes are found in the elephant shark genome, and two OPN3 genes are found in the whale shark genome (NCBI), we did not detect parapinopsin, OPN3, TMT2, or TMT3 transcripts in our shark or ray retinas, although we did detect very low levels of partial TMT1 sequences in the eyes of four species (supplementary table S3, Supplementary Material online). A recent study on the lantern shark Etmopterus spinax was also unable to detect OPN3 in the retina, but found that it expressed in the skin (Delroisse et al. 2018). By way of comparison, we did find low levels of partial OPN3 transcripts in the eyes of the lamprey Geotria australis and the bowfin Amia calva (supplementary table S3, Supplementary Material online). Although the sequencing data and microspectrophotometric measurements provide good evidence for the presence of particular opsins in the retina, sequencing of genomic DNA will be required to confirm any loss of opsin genes. Similarly, immunohistochemistry or in situ hybridization experiments will be required to localize the expression of pinopsin in the retina of the bamboo shark and elucidate its role in visual sensitivity.

Phototransduction Cascade for RH2 Opsin-Based Visual Pigments in Cartilaginous Fishes

Through our transcriptome analyses, we also identified the sequences for proteins involved in the phototransduction cascade that links photoactivation of the visual pigment with photoreceptor signaling. In gnathostomes, the RH2 opsin is found in morphological cones, and it is widely assumed that RH2 couples to the cone transduction cascade. This linkage has been established in the nocturnal gecko (Zhang et al. 2006), but currently there is little in the way of hard evidence for other gnathostome species. The Carcharhiniformes represent an interesting case, where our transcriptome data provide a clue. As discussed above, all cartilaginous fishes have lost the SWS1 and SWS2 opsin genes, and in addition our results (in combination with database searches) show that the Carcharhiniformes have additionally lost the LWS opsin; thus, the only remaining "nonrod" visual opsin is RH2. Supplementary table S4, Supplementary Material online, lists the transcript levels we measured in the four species of cartilaginous fishes for the three main protein classes (opsin, transducin, and PDE6) mediating the activation steps of phototransduction. For the gray reef shark, C. amblyrhynchos, where RH2 is the only nonrod visual opsin, there are transcripts for the cone isoforms GNAT2 and PDE6C. Furthermore, the levels of transcripts for the RH2, GNAT2, and PDE6C genes are each at least 100× lower than for the corresponding rod isoforms, RH1, GNAT1, PDE6A, and PDE6B, which reflects the fact that there are considerably fewer cones than rods in the retina. These results support the idea that in the gray reef shark retina, RH2 couples to the cone phototransduction cascade, in conformity with the case presumed in other gnathostome species. A hierarchical cluster analysis
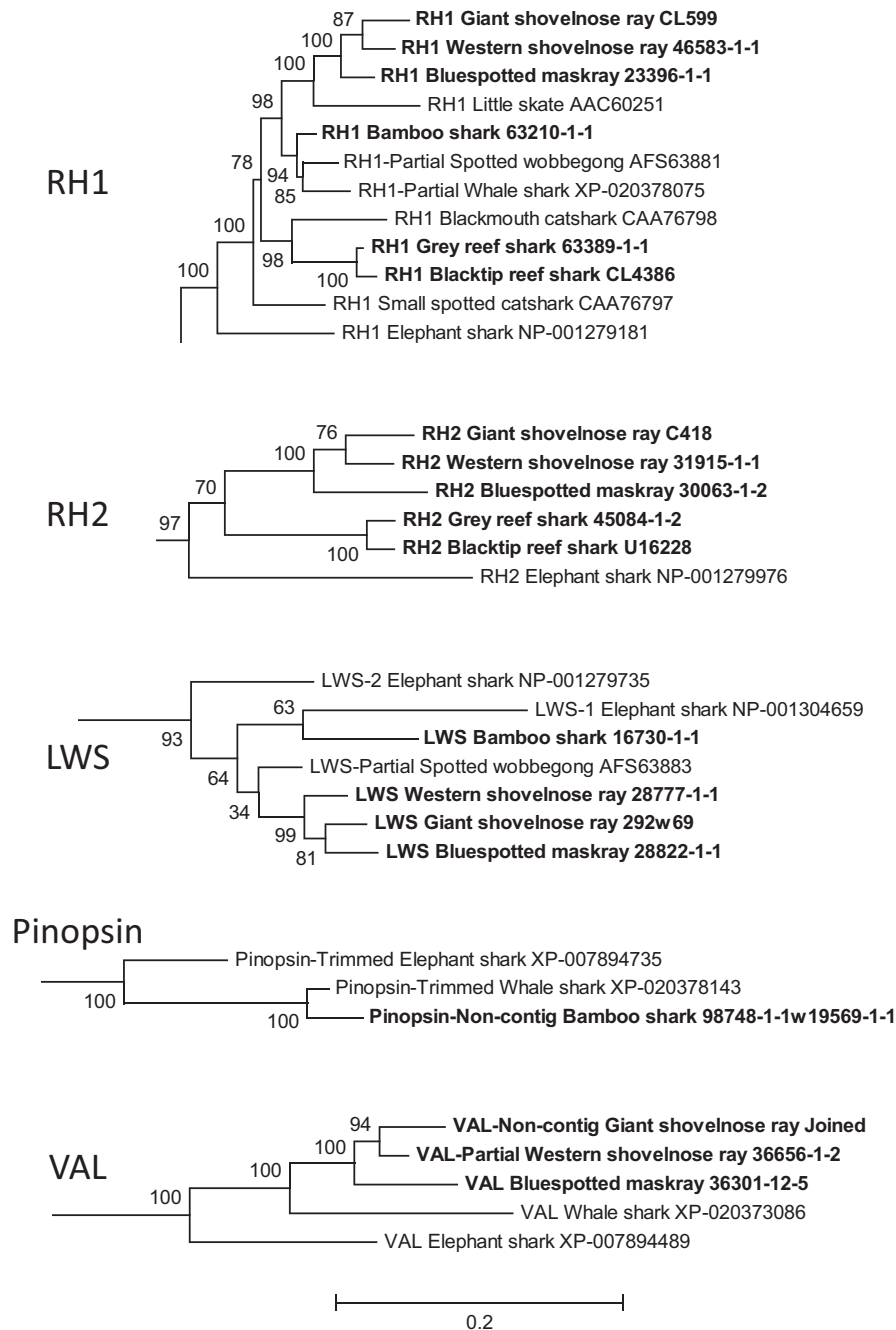
FIG. 5. Subtrees containing sequences from cartilaginous fishes, extracted from supplementary figure S2, Supplementary Material online. Bold font denotes newly reported sequences. Scale bar denotes amino acid substitutions per site.

of the gene expression data supports this association (supplementary fig. S3, Supplementary Material online). This scenario in gnathostomes differs from the situation that we recently proposed for agnathan vertebrates, where there is suggestive evidence that RH2 couples to GNAT1 and the rod cascade (Lamb and Hunt 2017).

Spectral and Functional Tuning of Visual Pigments

The absorbance spectrum of every photoreceptor outer segment measured using microspectrophotometry in this study was accurately fitted by an A_1 visual pigment template as devised by Govardovskii et al. (2000) with an appropriate value for the λ_{max}; see examples of the fits in figures 2 and 3. Moreover, we did not find transcripts for cytochrome P450 family 27 subfamily c member 1 (Cyp27c1)—which drives the production of vitamin A_2 and its derivatives from vitamin A_1, and is therefore necessary for the generation of A_2 visual pigments (porphyropsins based on 3,4-didehydroretinal) (Enright et al. 2015)—in any of the ray or shark transcriptomes analyzed in this study. We therefore conclude that all of the visual pigments we measured in these shark and ray species contained only the vitamin A_1 variant of the retinal chromophore. Accordingly, all differences in the spectral absorption properties of the visual pigments measured in this

study can be attributed solely to differences in the amino acid sequence of the opsin proteins, and are not confounded by the presence of a mixture of the A_1 and A_2 chromophores as seen in some other shark species, such as the bull shark *C. leucas* (Hart et al. 2011) and the lemon shark *Negaprion brevirostris* (Cohen et al. 1990). In table 3, we have listed the residues found at key tuning sites, both for our newly sequenced visual opsins and for sequences from other elasmobranch species, together with several reference visual opsin sequences. We have additionally tabulated the values of λ_{max} found by MSP where available. By analyzing these data, it should be possible in principle to determine the role of residues at different sites on the spectral tuning of the pigments.

RH1 (Rod) Opsin

Vertebrate RH1 visual pigments have λ_{max} values ranging from ∼475 to ∼525 nm when conjugated with the A_1 chromophore (Hunt et al. 2001). The residues present at sites 83, 122, 164, 207, 211, 261, 265, 269, 292, 295, and 308 (bovine rhodopsin numbering) in the RH1 opsin are thought to be particularly important for determining the λ_{max} of the visual pigment (Yokoyama 2000). Among the four species of ray examined here, the rod λ_{max} varies from 497 nm in the bluespotted maskray to 504 nm in the giant shovelnose ray, with the other two species (western shovelnose ray and little skate) within this range (table 3). As the amino acid residues at the 11 key tuning sites for RH1 are identical for these four species (table 3), this minor variability in λ_{max} may be due to measurement error or differences in residues at other sites that may produce small spectral shifts, for example, site 299 (Dungan and Chang 2017; Musilova et al. 2019).

Among the shark species for which we have both spectral and sequence data for RH1 opsins (table 3), there is greater variation in λ_{max}, ranging from 478 nm in the whale shark to 505 nm in the blacktip reef shark. For the spotted wobbegong, the shortwave-shifted λ_{max} of 484 nm has been attributed in part to an Ala292Ser substitution (Theiss et al. 2012), a change that generates a 10-nm shortwave shift in bovine RH1 (Janz and Farrens 2001); an identical substitution is present in blackmouth catshark RH1, which has a λ_{max} at 482 nm. Moreover, there is an Asp83Asn substitution in the blackmouth catshark and the velvet belly lanternshark RH1 pigments, a change that generates a ∼6-nm shortwave shift in bovine RH1 (Nathans 1990a) and, together with Ala292Ser, explains the shortwave-shifted λ_{max} values in the pigments of both species. Surprisingly, neither of these substitutions is present in whale shark RH1, which is the most shortwave-shifted shark RH1 pigment according to measurements made using recombinant opsin reconstituted with an A_1 chromophore (Hara et al. 2018). In fact, when comparing 46 known tuning sites identified across all opsin types (Takahashi and Ebrey 2003; Takenaka and Yokoyama 2007; Yokoyama 2008), the whale shark RH1 opsin differs from the bamboo shark RH1 opsin (λ_{max} 500 nm) only by having Ala instead of Thr at site 94. Ala94 is characteristic of SWS2 opsins, and in killifish SWS2 an Ala94Cys substitution causes a shortwave shift of

16 nm (Yokoyama et al. 2007). In human RH1, mutations at site 94 affect the interaction between the Schiff base (which binds 11-*cis* retinal to the opsin at Lys296) and its counterion Glu113, and thus alter the thermal stability of the pigment (Janz and Farrens 2004). Site-directed mutagenesis experiments will be required to establish whether site 94 affects the spectral tuning of the whale shark RH1 pigment.

Of the remaining six shark species for which both sequence and spectrophotometric data are available for RH1 opsins (table 3), the residues at the 11 putative key tuning sites are identical, but the λ_{max} values (all obtained by MSP) vary from 496 nm in the small spotted catshark to 505 nm in the blacktip reef shark. The spread of λ_{max} values suggests that some of this variation is real, but it cannot be attributed to substitutions at the known major tuning sites for RH1 opsins and, as with the whale shark, additional tuning sites may be responsible.

RH2 Opsin

Vertebrate RH2 visual pigments have λ_{max} values ranging from ∼440 to ∼530 nm when conjugated with the A_1 chromophore (Hart et al. 2008; Davies et al. 2009a). The RH2 pigments of elasmobranchs appear to span this range but fall into two distinct spectral groups: 1) those with λ_{max} values ∼450–481 nm in rays (with S-cones); and 2) those with λ_{max} values ∼528–534 nm in sharks (with L-cones). Amino acid residues at sites 83, 97, 122, 207, 292, 295 (bovine rhodopsin numbering) within the RH2 opsin are thought to be particularly important for determining the λ_{max} of the visual pigment, with other sites (including 49, 52, 86, 164) having more limited effects (Takenaka and Yokoyama 2007). Phylogenetic analyses suggest that the ancestral RH2 opsin had Asp83, Tyr 97, Glu122, Met207, Ala292 and Ser295, and a λ_{max} between ∼499 and 520 nm (Davies, Cowing, et al. 2007; Takenaka and Yokoyama 2007). The potential role of these sites in the spectral tuning of shark and ray RH2 pigments may be assessed, therefore, by comparison with other opsin sequences, as follows.

The three ray species for which sequence and microspectrophotometric data are available have λ_{max} values that are substantially shortwave-shifted to 476 nm in the bluespotted maskray, 477 nm in the giant shovelnose ray, and 460 nm in the western shovelnose ray (table 3). All three ray species have Asn rather than Asp at site 83. In bovine RH1, the substitution Asp83Asn shortwave-shifts the λ_{max} of the rod pigment (498 nm) by 6 nm to 492 nm (Nathans 1990b), but in the American chameleon *Anolis carolinensis* the same substitution causes no spectral shift in the λ_{max} (496 nm) of the RH2 pigment (Takenaka and Yokoyama 2007). The significance of this site for spectral tuning in ray RH2 pigments is, therefore, unclear.

Substitutions at site 122 and 207, on the other hand, are known to cause substantial shifts in the λ_{max} of both RH1 and RH2 pigments. The substitution Glu122Gln causes a shortwave shift of ∼19–21 nm in bovine and chicken RH1 (Nathans 1990b; Imai et al. 1997) and the reverse substitution Gln122Glu causes a longwave shift of 13–16 nm in the RH2

pigments of the Comoran coelacanth *Latimeria chalumnae*, American chameleon *An. carolinensis*, Tokay gecko *Gekko gecko*, and chicken (Imai et al. 1997; Yokoyama et al. 1999; Takenaka and Yokoyama 2007). The substitution Leu207Met causes a 6-nm longwave shift in the coelacanth visual pigment (Yokoyama et al. 1999) and, as with site 122, the reverse substitution might be expected to generate a shift of similar magnitude toward shorter wavelengths. Compared with the putative ancestral RH2 pigment (λ_{max} ~499 nm) and bovine rhodopsin (λ_{max} 499 nm), the bluespotted maskray and the giant shovelnose ray both share the substitutions Glu122Gln and Met207Leu, and the additive effect of these substitutions could be sufficient to explain the observed shortwave shift in λ_{max} to ~476 nm.

The western shovelnose ray RH2 pigment also has Gln122 and Leu207, but its λ_{max} at 460 nm is shifted even further toward shorter wavelengths. Inspection of the residues at other putative spectral tuning sites identified for RH2 and/or RH1 opsins as well as other opsin classes (Takahashi and Ebrey 2003; Takenaka and Yokoyama 2007) reveals that the three rays differ at only three of these sites: 87, 118, and 211. At site 87, the bluespotted ray differs from the other rays by having Val rather than Ile, but there is only ~1nm difference (the wavelength accuracy of the MSP) between the λ_{max} values of the bluespotted ray and the giant shovelnose ray, and this is also a conservative substitution that would not be expected to cause a significant spectral shift. By contrast, the western shovelnose ray has Ala118 and His211, whereas the bluespotted maskray and giant shovelnose ray have Thr118 and Tyr211 (table 3). The substitutions His211Cys and His211Phe cause shortwave shifts of 5 and 3 nm, respectively, in bovine RH1 (Nathans 1990b), but the effect of Tyr211His on RH2 pigments is unknown. On the other hand, in bovine RH1 a Thr118Ala substitution causes a 16 to 18nm shortwave shift in λ_{max} (Janz and Farrens 2001). This substitution alone could potentially explain the additional shortwave shift in the western shovelnose ray RH2 pigment.

The RH2 pigments in all the shark species for which MSP data are available show significant longwave shifts (of ~51–74 nm) compared with those of the rays, with λ_{max} values ranging from ~528 nm in the blacktip reef shark to ~534 nm in the pigeye shark (table 2). Of these species, sequence data are only available for the blacktip reef shark and the common blacktip shark (table 3). Compared with the proposed ancestral RH2 pigment (see above), the shark RH2 pigments differ at the major tuning sites only by a Ser295Ala substitution. In bovine RH1, the reverse Ala295Ser substitution causes a shortwave shift of 2–5 nm (Lin et al. 1998; Janz and Farrens 2001). Consistent differences between the ray and shark RH2 pigments at other known tuning sites are Leu49Gly, Gly164Ala, His197Lys, and Ala269Thr; of these only the latter is known to produce significant spectral shifts, with Ala269Thr producing a ~14nm longwave shift in both RH1 and M/LWS pigments (Neitz et al. 1991; Chan et al. 1992).

Photokinetics of RH1 and RH2 Opsins

Several substitutions are thought to impact on the photokinetics and functionality of the RH1 rod and RH2 cone pigments. In particular, the residues present at sites 122 and 189 are thought to impact directly on the rate of decay of the photoproduct metarhodopsin II and on the rate of pigment regeneration, with the combination of Glu122/Ile189 as present in RH1 pigments showing much reduced rates compared with Gln122/Pro189 as more generally present in RH2 and other cone pigments (Imai et al. 1997; Kuwayama et al. 2002). RH1 rod pigments evolved from ancestral cone-like "RH" pigments that would have been expressed in cones (Okano et al. 1992; Lamb and Hunt 2017), and the substitutions Gln122Glu and Pro189Ile are, therefore, considered to be adaptive for scotopic vision, possibly by increasing pigment stability and thereby reducing the spontaneous rate of thermal isomerization. On the other hand, the increased lifetime of the photoproduct metarhodopsin II will not directly affect photosensitivity, because the lifetime of the active form (R*) is determined by the much faster reactions of phosphorylation and arrestin binding (Lamb and Kraft 2016).

For shark and ray RH1 pigments, Glu122 is universally present whereas the RH2 pigments differ, with Gln122 present in rays and Glu122 present in the two shark species for which sequences are available (gray reef shark and blacktip reef shark). The RH2 pigments of both sharks and rays have Pro189, as for other cone opsins, whereas the RH1 pigments have either Ile189 or Val189 (Val is a conservative replacement for Ile), as in other rod opsins. Interestingly, the only RH2 sequence with Glu122, and for which the spectrum has been measured (blacktip reef shark), is longwave-shifted with a peak at 528 nm. The other shark RH2 opsins are longwave-shifted (table 2), and if sequence data showed them to have Glu122 then this would suggest that the "rod-like" Glu122 residue in these RH2 cone opsins may well serve a purpose in helping to stabilize the RH2 opsin against the thermal instability that typically results from a longwave shift in spectral peak (Ala-Laurila et al. 2004).

Residues at several other sites are also thought to influence pigment photokinetics, including sites 83, 119, 123, 124, 292, and 299 (Dungan and Chang 2017; Castiglione and Chang 2018). All of the sharks and rays for which RH1 sequence data are available are conserved at site 119 (Leu), but differ at sites 123 and 124 (supplementary file 1, Supplementary Material online) with substitutions (e.g., Ala124Ser in the bluespotted maskray) that in bovine RH1 affect the rate of release of all-*trans* retinal from metarhodopsin II and thus the time taken to regain photosensitivity (Castiglione and Chang 2018). It is likely that many substitutions affect both the spectral and kinetic properties of these pigments through epistatic interactions, and functional studies will be required to properly assess the impact on pigment function (Dungan and Chang 2017).

LWS Opsin

Vertebrate LWS visual pigments have λ_{max} values ranging from 499 to 571 nm when conjugated with the A_1

chromophore (Okano et al. 1989; Davies et al. 2009a), and spectral shifts over this range are attributed primarily to a combination of amino acid substitutions at just five sites, 164 (180), 181 (197), 261 (277), 269 (285), and 292 (308) (bovine rhodopsin numbering, with human LWS opsin numbering in parentheses) (Yokoyama and Radlwimmer 2001). A phylogenetic analysis of vertebrate LWS pigments suggests that the ancestral LWS opsin had Ser164, His181, Tyr261, Thr269, and Ala292 and, based on the known spectral shifts that occur as a result of substitutions at one or more of those five sites, this pigment would be expected to have a λ_{max} at ~560 nm (Yokoyama et al. 2008). Indeed, the LWS opsin of giant shovelnose ray has exactly this complement of amino acids at these five sites and a λ_{max} at 561 nm (table 3).

The other two ray species for which LWS sequence data are available are the bluespotted maskray and western shovelnose ray, which have λ_{max} values at 552 and 557 nm, respectively. These pigments have a Tyr261Phe substitution that has been shown to generate 7–10 nm shortwave shifts in primate (Neitz et al. 1991; Asenjo et al. 1994) and elephant shark LWS pigments (Davies et al. 2009a), so this would account for the shift in λ_{max} in both species compared with the giant shovelnose ray.

A similar substitution is found in the LWS opsin of the spotted wobbegong (λ_{max} 553 nm) and the ornate wobbegong (λ_{max} 561 nm) (table 2), although only the former species shows a shortwave shift. The only other shark species shown to possess an LWS pigment and for which spectral data are available is the brown-banded bamboo shark with a λ_{max} at 532 nm, which is considerably more shortwave-shifted than the LWS pigments of the rays and the wobbegong sharks. The bamboo shark LWS pigment has (in addition to a Tyr261Phe) a Thr269Ala substitution that is known to cause a shortwave shift of ~15–16 nm in LWS pigments (Neitz et al. 1991; Asenjo et al. 1994), so together with Tyr261Phe, this would be expected to produce an LWS pigment with a λ_{max} at ~534 nm (Yokoyama et al. 2008). Based on this limited survey of seven species, the spectral tuning of elasmobranch LWS pigments appears to adhere closely to the "five-sites rule" (Yokoyama and Radlwimmer 2001).

Discussion

In this study, we provide the most detailed picture yet of the diversity of C-opsins expressed in the retinas of elasmobranchs. Our findings are relevant for understanding the evolution of cone-based chromatic vision across vertebrates.

Loss of Visual Opsins in Chondrichthyans

The five major classes of visual opsin genes present in vertebrates (SWS1, SWS2, RH1, RH2, and LWS) evolved prior to the divergence of the agnathan lampreys from the gnathostomes over 540 Ma (Collin et al. 2003; Pisani et al. 2006). Given the complement of opsin genes present in extant cartilaginous (chondrichthyan) fishes, it would appear that the SWS1 and SWS2 opsin genes were lost from this lineage following its separation from the bony fishes (Osteichthyes) ~460 Ma (Inoue et al. 2010) and prior to the divergence of the holocephalan (chimeras) and the elasmobranchs (sharks, skates,

and rays) ~420 Ma (Renz et al. 2013). Thus, it seems likely that only the RH1, RH2, and LWS opsin genes were retained in ancestral chondrichthyans, with a subsequent gene duplication within the holocephalan lineage giving rise to two copies of the LWS opsin gene in the elephant shark Callorhinchus milii (Davies et al. 2009a).

Within the elasmobranchs, representatives from seven families of ray (Batoidae) have retained both the RH2 and LWS cone opsin genes in addition to RH1, based on a combination of molecular and microspectrophotometric data from this study and previous studies (Hart et al. 2004; Theiss et al. 2007; Bedore et al. 2013). The presence of two spectrally distinct cone types provides the neural substrate for dichromatic color vision, and behavioral experiments in the giant shovelnose ray demonstrate that they can discriminate color (Van-Eyk et al. 2011). The presence of cone pigments and color vision in the other major groups of batoids, the skates and sawfishes, is unknown, although at least two species of skate are thought to possess rod-only retinae (Ripps and Dowling 1990). The retention of a dichromatic color vision system resembles that found in many marine teleosts, which are typically di- or trichromatic (Loew and Lythgoe 1978). Broadly speaking, color discrimination may be useful for behaviors such as prey detection, predator avoidance, and mate choice. However, most rays likely use other senses such as electroreception to localize their benthic prey (Kalmijn 1971) and, with relatively few exceptions, rays are not particularly colorful or sexually dimorphic. Given that many ray species spend considerable periods of time resting on or partially buried in the substrate, color vision may instead aid in the detection of approaching overhead predators through either enhancement of visual contrast or elimination of achromatic flicker (Sabbah and Hawryshyn 2013).

The situation in the sharks (Selachii) appears to be more complex. Although all sharks studied to date have retained the rod-based RH1 opsin, only a single cone opsin has been found in any given species, and the molecular and microspectrophotometric data available suggest that this condition may be common to at least five shark families from three different orders. Thus, many sharks appear to be cone monochromats, although it is important to note that very few of the ~500 extant shark species (Compagno et al. 2005) have been studied. Intriguingly, it appears that although the orectolobiform families, that is, the bamboo (Hemiscylliidae), wobbegong (Orectolobidae), and whale sharks (Rhincodontidae), have retained the LWS cone opsin gene, the Carcharhiniformes, that is, the requiem sharks (Carcharhinidae), and the heterodontiforms, that is, the zebra bullhead shark (Heterodontidae), have retained the RH2 cone opsin gene; therefore, a reversion from cone dichromacy to cone monochromacy appears to have evolved independently in sharks at least three times (fig. 6).

Recent phylogenies based on morphological characters and molecular data show a close relationship between the Orectolobiformes and the Carcharhiniformes. Several analyses support the position of the Orectolobiformes as sister to a group comprising the Lamniformes and Carcharhiniformes with an estimated time of divergence of ~179 Ma
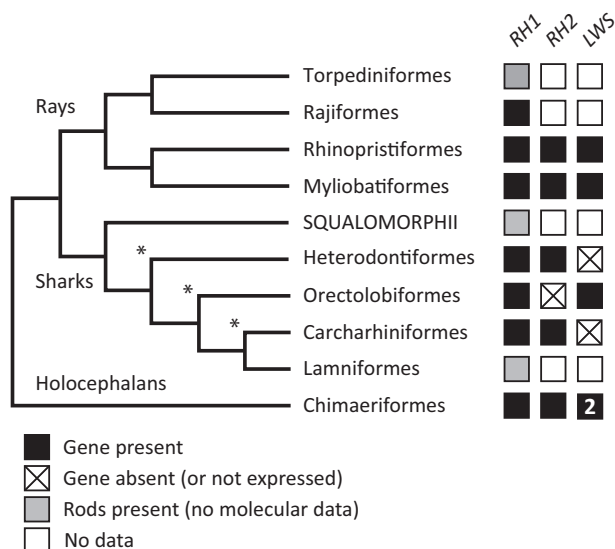
Fig. 6. Schematic phylogeny of shark and rays showing the presence and absence of visual opsin genes in different taxa. Asterisks (*) indicate lineages where a reversion to cone monochromacy has occurred from a presumed dichromatic ancestor. For comparison, the visual opsin complement of the elephant shark (a holocephalan) is shown and indicates a duplication of the LWS opsin gene.

(Heinicke et al. 2009; Naylor et al. 2012; Sorenson et al. 2014), whereas others find support for a closer relationship between the Orectolobiformes and the Carcharhiniformes, with the Lamniformes as a sister group (Vélez-Zuazo and Agnarsson 2011). Given that the common ancestor of the Orectolobiformes and the Carcharhiniformes must have possessed both RH2 and LWS, this raises the possibility that shark orders that diverged earlier, including the Heterodontiformes and all the Squalimorphii, may contain representatives that possess both cone opsins types. The only heterodontiform shark for which sequence data are available, the zebra bullhead shark, possesses just the RH2 opsin gene (Hara et al. 2018), which implies that this lineage may have independently lost the LWS opsin gene after it split from the common ancestor of the Orectolobiformes and Charchariniformes ~274 Ma (Sorenson et al. 2014). The Squalimorphii are a diverse group with many strongly nocturnal or deep diving species that possess an all-rod (RH1) retina, as in the velvet belly lanternshark E. spinax (Claes et al. 2014; Delroisse et al. 2018), but also others where cones are present, as in the spiny dogfish Squalus acanthias (Stell 1972), and so it is possible that cone dichromat sharks do exist.

Additional sequences will be required to provide a more complete picture of elasmobranch opsin evolution, and preliminary evolutionary analyses indicate differences between opsin types that may be functionally relevant. Supplementary table S5, Supplementary Material online, lists estimates of nonsynonymous (dN) and synonymous (dS) substitution rates for shark and ray RH1, RH2, and LWS opsins. In both sharks and rays, the dN/dS values for RH2 are significantly higher than for RH1 or LWS ($P < 0.01$ for all comparisons; one-tailed Student's t-test). This would imply that a greater proportion of the substitutions in the RH2 gene generate coding changes in amino acids, indicating that the RH2 opsin tolerates more sequence changes than the RH1 or LWS opsins and potentially has a higher divergence rate. However, these results are based on very few opsin sequences and should be interpreted with caution.

The retention of just a single cone visual pigment in sharks with λ_{max} ~520–540 nm mirrors the situation found in extant cetaceans and pinnipeds, which have lost the ancestral mammalian SWS1 opsin gene class (Newman and Robinson 2005; Fasick et al. 2011). It has been suggested, among other hypotheses, that this situation arose in marine mammals as an adaptation to the greener coastal waters they inhabited during their transition to the water (Peichl et al. 2001). However, despite an earlier report indicating that loss of the SWS1 opsin gene might have occurred prior to the divergence of the two extant cetacean lineages (Levenson and Dizon 2003), a more recent analysis suggests that it occurred independently in the stem mysticete (baleen whale) and odontocete (toothed whales) lineages after both lineages had already moved into the pelagic realm (Meredith et al. 2013). Thus, rather than being the result of a "coastal bottleneck" during evolution, a reversion to cone monochromacy independently in several primarily and secondarily aquatic taxa suggests that color vision is of little value to many large marine predators.

Color vision requires opponent neural mechanisms that compare the output of different spectral photoreceptor types. Inhibitory interactions between photoreceptor channels can decrease the signal-to-noise ratio and, therefore, may degrade the ability to detect subtle differences in image contrast (Kelber and Roth 2006); in dim light, a monochromatic visual system may be capable of discriminating a greater number of distinct reflectance spectra than a di- or trichromatic one, purely based on intensity differences (Vorobyev 1997). Color vision also degrades spatial acuity, especially when the spectral peaks of the photoreceptor channels are widely separated, because the signals from different cones types will reflect both spectral and intensity differences in the image (Roorda et al. 2001). For this reason, many animals rely predominantly on a single spectral channel to convey high-resolution achromatic spatial information (Lind and Kelber 2011), but of course any other spectral cone types are then taking up valuable retinal "real estate" that could otherwise be used to improve resolution in bright light (i.e., more receptors per degree of visual angle) and/or reduce noise in dim light (i.e., through neural summation). Due to absorption, reflection, and scattering by the water itself and any dissolved or suspended substances, most aquatic habitats are characterized by low visual contrast. Moreover, many sharks are active both night and day and must therefore operate under a wide range of light intensities. It is likely therefore that sharks are often operating close to the threshold of their visual capabilities where the disadvantages of color vision circuitry might be detrimental to survival.

Although cone monochromacy and thus a lack of cone-based color vision would appear to be common in sharks, it is possible that neural signals from the spectrally distinct rod and cone photoreceptors might be compared under certain

(i.e., mesopic) illumination conditions, when both receptor types are functional (Hart et al. 2011). Such an arrangement might provide a rudimentary form of dichromatic color vision, as reported in some human blue-cone monochromats (Reitner et al. 1991), and indeed cone–rod (UV–green) color opponent ganglion cells have been identified in the mouse retina (Joesch and Meister 2016). However, previous behavioral studies have failed to demonstrate color vision in either carcharhinid (Cohen 1980) or hemiscyllid sharks (Schluessel et al. 2014), which tallies with the opsin and microspectrophotometric data and suggests that rod–cone based color vision is not operational in these species. These studies reflect similar findings in other cone monochromats, such as the harbor seal *Phoca vitulina* (Scholtyssek et al. 2015) and the nocturnal owl monkey *Aotus trivirgatus* (Jacobs et al. 1993).

Spectral and Functional Tuning of Elasmobranch Visual Pigments

Figure 7 summarizes the spectral distribution of rod and cone pigments measured in elasmobranchs. Substantial variation in rod (RH1) pigment λ_{max} is limited to the sharks, with the whale shark shortwave-shifted to $\sim$478 nm and the bull shark pigment longwave-shifted to 518 nm. Shortwave-shifted RH1 rod pigments are typically found in aquatic species that live at depth in clear waters, where the light available for vision is restricted to a relatively narrow waveband from $\sim$460 to $\sim$490 nm (Denton and Warren 1956; Hunt et al. 1996, 2001; Douglas and Partridge 1997; Hope et al. 1997). Visual pigments with λ_{max} values matched to the most abundant wavelengths, or those transmitted best, would be adaptive for maximizing visual sensitivity and visual range under these conditions (Lythgoe 1968). The elasmobranchs measured and sequenced in this study are predominantly shallow dwelling, spending most of their time in waters that are tens rather than hundreds of meters deep, and their rod pigments fall into a typical range for similar marine species, with λ_{max} values close to 500 nm (Munz and McFarland 1973). The exception is the spotted wobbegong shark, which is also considered a shallow water species but has a rod pigment λ_{max} at 484 nm that is more characteristic of deep-dwelling species such as the black mouth catshark. Factors other than depth and water color may influence the spectral tuning of visual pigments; for example, thermal stability of a visual pigment is related to its λ_{max}, with shortwave-shifted pigments being more stable and thereby generating less dark noise in the photoreceptors (Ala-Laurila et al. 2007). The λ_{max} of the rod pigment is, therefore, likely to be a compromise between spectral and thermal considerations, and as the spotted wobbegong is a largely nocturnal hunter it may benefit from the enhanced signal-to-noise ratio provided by a shortwave-shifted rod pigment.

The RH2 pigments of rays have λ_{max} values that range from 450 nm in the spotted eagle ray to 481 nm in the common stingray. The former species is the most pelagic studied and the shortwave-shifted λ_{max} may be an adaptation to
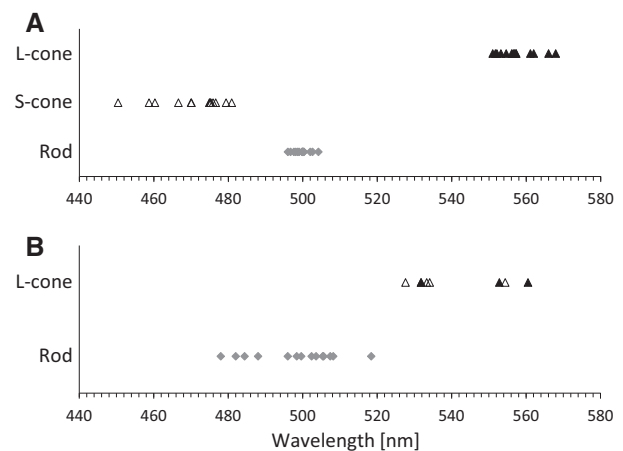

Fig. 7. Spectral distribution of rod and cone visual pigment λ_{max} values in rays (*A*) and sharks (*B*), incorporating data from microspectrophotometry (tables 1 and 2) and spectrophotometric measurements of reconstituted visual pigments from recombinant opsin (table 3). The known or predicted opsin class expressed in each photoreceptor type is indicated (RH1, filled diamonds; RH2, open triangles; LWS, filled triangles).

maximize visual sensitivity in its bluer open water habitat compared with the more turbid, greener coastal waters occupied by the other benthic species; a similar trend has been observed in the twin/double cone pigments of teleost fishes occupying a range of water types (Lythgoe et al. 1994). By contrast, shark RH2 visual pigments have λ_{max} values that are substantially longwave-shifted to $\sim$530 nm and indeed are among the most longwave-shifted RH2 pigments yet measured. As different shark species possess either the RH2 or the LWS pigment but not both, the longwave shift in the RH2 pigment would appear to be an adaptation to the loss of the LWS pigment, to give a similar spectral range to the species with LWS pigments. Although the spectral tuning of shark and ray LWS pigments follows closely the five-sites rule proposed by Yokoyama and Radlwimmer (2001), the mechanisms of spectral tuning in the RH2 pigment are less clear and, given the observed variation in λ_{max}, elasmobranchs may represent a useful taxon for exploring further the adaptability of RH2 opsins.

Another striking feature of the shark RH2 pigments is that they possess Glu122, which is characteristic of rod RH1 pigments and is thought to result in slower rates of metarhodopsin II decay and pigment regeneration compared with canonical RH2 cone pigments with Gln122, as found in rays. Glu122 is thought to stabilize the visual pigment, resulting in a lower thermal activation rate and thus reduced dark noise (Yanagawa et al. 2015), thereby improving the signal-to-noise ratio of single-photon detection at the lowest ambient light levels. We speculate that the loss of the LWS opsin in some shark species necessitated a subsequent longwave shift in the RH2 pigment λ_{max} (from a spectral location close to that seen in extant rays and holocephalans) and that the inevitable increase in the thermal activation rate this would incur was mitigated somewhat by Gln122Glu.

Materials and Methods

Animals

Sharks and rays obtained from Australian waters under relevant wildlife permits (Department of Primary Industries General Fisheries Permits PRM03951I and PRM377271, Great Barrier Reef Marine Parks Authority Permits QS2003/CVL625 and G06/15528.1) were killed humanely in accordance with institutional Animal Ethics Committee approvals (UQ: SBMS/067/06/ARC, SBMS/205/07/ARC, SBMS/613/08/ARC; UWA: RA/3/100/917 and RA/3/100/1220). Animals were euthanized by immersion in a lethal concentration of fish anesthetic MS222 (ethyl 3-aminobenzoate methanesulfonate salt, 500 mg/l) followed by transection of the spinal cord, or decapitation. The elasmobranch species used for each aspect of the present study, their source, and relevant morphometric data are listed in supplementary table S1, Supplementary Material online.

Sequencing of Opsin Genes

Tissue Extraction

Eyes were removed postmortem, hemisected at the equator, and the posterior pole containing the retina was placed in RNA stabilization solution (RNAlater, Ambion). Samples were stored at room temperature for periods of up to a few days, but at −20 °C or −80 °C for longer periods. Opsin sequences were obtained from whole-transcriptome sequencing and also conventional RT-PCR, cloning and sequencing as described below. Using the three approaches, we report a total of 43 new mRNA sequences, which have been deposited at GenBank with accession numbers (MN519142–MN519184). The sets of reads from which the transcriptomes were assembled have been deposited at the NCBI Sequence Read Archive under SRA Study SRP062082.

Transcriptome Sequencing

Retinal tissue was processed for transcriptome sequencing on two next-generation sequencing platforms, one at the Australian National University (ANU; Canberra) Australian Cancer Research Foundation (ACRF) Biomolecular Resource Facility (BRF), and the other at the Beijing Genomics Institute (BGI; Shenzhen, China).

The methods used at ANU for obtaining eye transcriptomes are described in Lamb et al. (2016), and here we use transcripts from that work. Sequences were available for each of the following species obtained from Australian waters: western shovelnose ray, A. vincentiana; blue-spotted maskray, Neotrygon kuhlii (N. australiae); brown-banded bamboo shark, Chiloscyllium punctatum; gray reef shark, C. amblyrhynchos; broad-gilled hagfish, Eptatretus cirrhatus; pouched lamprey Geotria australis; and the short-headed lamprey, Mordacia mordax;. Sequences were also obtained from bowfin, Am. calva, and Florida gar, Lepisosteus platyrhincus. Searching of our transcriptomes was performed using a custom program, TriPyGDU (Lamb et al. 2016), and augmented using a BLAST server, SequenceServer (Priyam et al. 2015).

For sequencing at BGI, retinal total RNA was extracted using an Ambion mirVana miRNA Extraction kit (Life Technologies) following the manufacturer's instructions. Samples were shipped to China on dry ice for library preparation and sequencing on an Illumina HiSeq 2000 sequencing system. De novo assembly of reads into contiguous sequences was performed using Trinity (release-20121005; Grabherr et al. 2011). Assembled sequences were aligned against reference protein databases (NR, KEGG, Swiss-Prot, COG) using BlastX (Camacho et al. 2009). Sequences were obtained from the giant shovelnose ray Glaucostegus typus and the black-tip reef shark C. melanopterus.

Conventional Sequencing

Opsin sequences were obtained through conventional RT-PCR, cloning and sequencing from two additional shark species, the common blacktip shark, C. limbatus, and the dusky shark, C. obscurus. Retinal mRNA was extracted from homogenized retinal tissue using the RNeasy Mini Kit (Qiagen) and converted to cDNA using the QuantiTect Reverse Transcription Kit (Qiagen) following the manufacturers' instructions. The degenerate PCR primers used in nested-PCR to generate the LWS, SWS1, SWS2, RH2, and RH1 exon 2–4 partial sequences for the common blacktip shark C. limbatus and the dusky shark C. obscurus are the first four listed in table 1 of Davies et al. (2009). First round PCR products were generated using the HotStarTaq Plus Master Mix Kit (Qiagen) with AOASF1 (forward) and AOASR2 (reverse) primers under the following conditions: an initial denaturation of 94 °C for 5 min, 40 cycles of 94 °C for 30 s, 45 °C for 1 min, 72 °C for 1.5 min, and a final extension of 72 °C for 10 min. Resultant PCR products were diluted 1 in 10 and used as the template in a second-round heminested or full-nested PCR using the following primer combinations: 1) AOASF1 (forward) and AOASR1 (reverse); 2) AOASF2 (forward) and AOASR2 (reverse); and 3) AOASF2 (forward) and AOASR1 (reverse). Conditions for the second-round PCR were similar to the first-round PCR, except for the use of an annealing temperature of 50 °C (Davies et al. 2009b). Second-round PCR products were visualized by agarose gel electrophoresis, purified using the Wizard SV Gel and PCR Clean-Up System (Promega) and cloned into the pGEM-T Easy Vector (Promega) following the manufacturers' instructions. Colonies were screened by blue/white selection, and colony PCRs performed with T7 and SP6 primers to confirm the presence of inserts. Selected positive clones were cultured overnight at 37 °C in Luria-Bertani broth, and plasmid DNA was purified subsequently using the AxyPrep Plasmid Miniprep kit (Axygen). Inserts were sequenced using T7 or SP6 primers and a Big Dye Terminator v3.1 Cycle Sequencing kit on an Applied Biosystems 3730 DNA Analyzer (Australian Genome Research Facility, Brisbane and Perth).

Molecular Phylogenetic Analysis

Sequence Selection

In order to construct a phylogeny for vertebrate visual opsins, we aimed to select a representative set of gnathostome sequences, together with our new sequences for elasmobranch fishes, and all of the sequences that we could locate

for agnathan vertebrates. In addition to the five conventional classes of vertebrate "visual" opsin (RH1, RH2, SWS1, SWS2, LWS) and pinopsin, we also selected the long isoform of VAL, parapinopsin and parietopsin, with the consequence that parietopsin functioned as the outgroup. Using these sequences, the multiple sequence alignment was very tight (see supplementary file S1, Supplementary Material online). In preliminary analyses, we also tried using the more basal vertebrate C-opsins, OPN3 and the TMTs, as well as C-opsins from invertebrates (tunicates, lancelets, and protostomes) but we found that the resulting alignments appeared less secure, and so we restricted our final analysis to the vertebrate C-opsins listed above. We omitted a partial common blacktip shark RH1 sequence that (over its 100 residues) was identical to the full-length blacktip reef shark RH1 sequence. In addition, where we had sequences for Florida gar and spotted gar that were nearly identical, we omitted spotted gar. Altogether, we included 202 opsin sequences for alignment and tree inference.

Multiple Sequence Alignment and Tree Inference

We performed multiple sequence alignment of protein sequences using MAFFT (version 7.409) (Katoh and Standley 2013) with the L-INS-i method; we did not manually adjust any alignment and we always used the entire alignment. We made unconstrained maximum likelihood phylogenetic trees using IQ-Tree (Windows multicore version 1.7beta5) (Nguyen et al. 2015) using the ultrafast bootstrap approximation (Hoang et al. 2018) with 10,000 bootstrap replicates. Numbers at each node represent percentage support.

Microspectrophotometry

Animals were dark-adapted for up to 2 h prior to euthanasia. Eyes were removed under dim red light and all subsequent dissections were conducted under infrared light with the aid of infrared image converters (ElectroViewer 7215; Electrophysics Corporation, Fairfield, NJ). Retinal tissue was prepared for microspectrophotometry as described in detail elsewhere (Theiss et al. 2007; Hart et al. 2011). Briefly, eyes were hemisected, and small (1–2 mm^2) pieces of neural retina were dissected clear of the retinal epithelium. Retinal samples were mounted between No. 1 glass microscope coverslips in a drop of elasmobranch physiological saline solution containing 5–8% dextran (MW 282,000; Sigma D-7265). Transverse absorbance spectra (330–800 nm) were made of individual rod and cone outer segments using a single-beam, wavelength-scanning microspectrophotometer and analyzed using established methods described elsewhere (Hart 2004; Hart et al. 2011). The physical dimensions of spectrally identified outer segments were measured using a calibrated transparent overlay from images presented on the screen of the CCTV monitor used to view the preparations.

Supplementary Material

Supplementary data are available at *Molecular Biology and Evolution* online.

References

Ala-Laurila P, Donner K, Crouch RK, Cornwall MC. 2007. Chromophore switch from 11-cis-dehydroretinal (A2) to 11-cis-retinal (A1) decreases dark noise in salamander red rods. *J Physiol.* 585(1):57–74.

Ala-Laurila P, Pahlberg J, Koskelainen A, Donner K. 2004. On the relation between the photoactivation energy and the absorbance spectrum of visual pigments. *Vision Res.* 44(18):2153–2158.

Asenjo AB, Rim J, Oprian DD. 1994. Molecular determinants of human red/green color discrimination. *Neuron* 12(5):1131–1138.

Beaudry FEG, Iwanicki TW, Mariluz BRZ, Darnet S, Brinkmann H, Schneider P, Taylor JS. 2017. The non-visual opsins: eighteen in the ancestor of vertebrates, astonishing increase in ray-finned fish, and loss in amniotes. *J Exp Zool (Mol Dev Evol)*. 328(7):685–696.

Bedore CN, Loew ER, Frank TM, Hueter RE, McComb DM, Kajiura SM. 2013. A physiological analysis of color vision in batoid elasmobranchs. *J Comp Physiol A*. 199(12):1129–1141.

Bozzano A, Murgia R, Vallerga S, Hirano J, Archer S. 2001. The photoreceptor system in the retinae of two dogfishes, *Scyliorhinus canicula* and *Galeus melastomus*: possible relationship with depth distribution and predatory lifestyle. *J Fish Biol.* 59:1258–1278.

Brin KP, Ripps H. 1977. Rhodopsin photoproducts and rod sensitivity in the skate retina. *J Gen Physiol.* 69(1):97–120.

Camacho C, Coulouris G, Avagyan V, Ma N, Papadopoulos J, Bealer K, Madden TL. 2009. BLAST+: architecture and applications. *BMC Bioinformatics* 10(1):421.

Castiglione GM, Chang B. 2018. Functional trade-offs and environmental variation shaped ancient trajectories in the evolution of dim-light vision. *eLife* 7:e35957.

Chan T, Lee M, Sakmar TP. 1992. Introduction of hydroxyl-bearing amino acids causes bathochromic spectral shifts in rhodopsin. Amino acid substitutions responsible for red-green color pigment spectral tuning. *J Biol Chem.* 267:9478–9480.

Claes JM, Partridge JC, Hart NS, Garza-Gisholt E, Ho H-C, Mallefet J, Collin SP. 2014. Photon hunting in the twilight zone: visual features of mesopelagic bioluminescent sharks. *PLoS One* 9(8):e104213.

Cohen JL. 1980. Functional organization of the retina of the lemon shark (*Negaprion brevirostris*, Poey): an anatomical and electrophysiological approach [PhD thesis]. [Coral Gables (FL)]: University of Miami.

Cohen JL, Hueter RE, Organisciak DT. 1990. The presence of a porphyropsin-based visual pigment in the juvenile lemon shark (*Negaprion brevirostris*). *Vision Res.* 30(12):1949–1953.

Collin SP, Knight MA, Davies WL, Potter IC, Hunt DM, Trezise A. 2003. Ancient colour vision: multiple opsin genes in the ancestral vertebrates. *Curr Biol.* 13(22):R864–R865.

Compagno LJV, Didier DA, Burgess GH. 2005. Classification of chondrichthyan fish. In: Burgess GH, Cailliet GM, Camhi M, Cavanagh RD, Fordham SV, Fowler S, Musick J, Simpfendorfer CA, editors. Sharks, rays and chimaeras: the status of the chondrichthyan fishes. Status Survey. IUCN/SSC Shark Specialist Group. Gland (Switzerland)/Cambridge: IUCN – The World Conservation Union. p. 4–11.

Cortesi F, Musilová Z, Stieb SM, Hart NS, Siebeck UE, Malmstrøm M, Tørresen OK, Jentoft S, Cheney KL, Marshall NJ. 2015. Ancestral duplications and highly dynamic opsin gene evolution in percomorph fishes. *Proc Natl Acad Sci U S A*. 112(5):1493–1498.

Davies WIL, Collin SP, Hunt DM. 2012. Molecular ecology and adaptation of visual photopigments in craniates. *Mol Ecol.* 21(13):3121–3158.

Davies WL, Carvalho LS, Cowing JA, Beazley LD, Hunt DM, Arrese CA. 2007. Visual pigments of the platypus: a novel route to mammalian colour vision. *Curr Biol.* 17(5):R161–R163.

Davies WL, Carvalho LS, Tay BH, Brenner S, Hunt DM, Venkatesh B. 2009a. Into the blue: gene duplication and loss underlie color vision adaptations in a deep-sea chimaera, the elephant shark *Callorhinchus milii. Genome Res.* 19(3):415–426.

Davies WL, Collin SP, Hunt DM. 2009b. Adaptive gene loss reflects differences in the visual ecology of basal vertebrates. *Mol Biol Evol.* 26(8):1803–1809.

Davies WL, Cowing JA, Carvalho LS, Potter IC, Trezise AEO, Hunt DM, Collin SP. 2007. Functional characterization, tuning, and regulation of visual pigment gene expression in an anadromous lamprey. *FASEB J.* 21(11):2713–2724.

Deeb SS, Wakefield MJ, Tada T, Marotte L, Yokoyama S, Marshall Graves JA. 2003. The cone visual pigments of an Australian marsupial, the tammar wallaby (*Macropus eugenii*): sequence, spectral tuning, and evolution. *Mol Biol Evol.* 20(10):1642–1649.

Delroisse J, Duchatelet L, Flammang P, Mallefet J. 2018. *De novo* transcriptome analyses provide insights into opsin-based photoreception in the lantern shark *Etmopterus spinax. PLoS One* 13(12):e0209767.

Denton EJ, Warren FJ. 1956. Visual pigments of deep sea fish. *Nature* 178(4541):1059.

Douglas RH, Partridge JC. 1997. On the visual pigments of deep-sea fish. *J Fish Biol.* 50(1):68–85.

Dungan SZ, Chang B. 2017. Epistatic interactions influence terrestrial–marine functional shifts in cetacean rhodopsin. *Proc R Soc B.* 284(1850):20162743.

Enright JM, Toomey Matthew B, Sato S-Y, Temple Shelby E, Allen James R, Fujiwara R, Kramlinger Valerie M, Nagy Leslie D, Johnson Kevin M, Xiao Y. 2015. Cyp27c1 red-shifts the spectral sensitivity of photoreceptors by converting vitamin A1 into A2. *Curr Biol.* 25(23):3048–3057.

Eschmeyer WN, Fricke R, van der Laan R. 2016. Catalog of fishes: genera, species, references. Available from: http://researcharchive.calacademy.org/research/ichthyology/catalog/fishcatmain.asp (accessed September 29, 2016).

Fasick JI, Bischoff N, Brennan S, Velasquez S, Andrade G. 2011. Estimated absorbance spectra of the visual pigments of the North Atlantic right whale (*Eubalaena glacialis*). *Mar Mamm Sci.* 27(4):E321–E331.

Fasick JI, Robinson PR. 1998. Mechanism of spectral tuning in the dolphin visual pigments. *Biochemistry* 37(2):433–438.

Govardovskii VI, Fyhrquist N, Reuter T, Kuzmin DG, Donner K. 2000. In search of the visual pigment template. *Vis Neurosci.* 17(4):509–528.

Grabherr MG, Haas BJ, Yassour M, Levin JZ, Thompson DA, Amit I, Adiconis X, Fan L, Raychowdhury R, Zeng Q, et al. 2011. Full-length transcriptome assembly from RNA-Seq data without a reference genome. *Nat Biotechnol.* 29(7):644.

Gruber SH, Loew ER, McFarland WN. 1990. Rod and cone pigments of the Atlantic guitarfish, *Rhinobatos lentiginosus* Garman. *J Exp Zool.* 256(S5):85–87.

Hara Y, Yamaguchi K, Onimaru K, Kadota M, Koyanagi M, Keeley SD, Tatsumi K, Tanaka K, Motone F, Kageyama Y, et al. 2018. Shark genomes provide insights into elasmobranch evolution and the origin of vertebrates. *Nat Ecol Evol.* 2(11):1761–1771.

Hart NS. 2004. Microspectrophotometry of visual pigments and oil droplets in a marine bird, the wedge-tailed shearwater *Puffinus pacificus*: topographic variations in photoreceptor spectral characteristics. *J Exp Biol.* 207(7):1229–1240.

Hart NS, Bailes HJ, Vorobyev M, Marshall NJ, Collin SP. 2008. Visual ecology of the Australian lungfish (*Neoceratodus forsteri*). *BMC Ecol.* 8(1):21.

Hart NS, Lisney TJ, Collin SP. 2006. Visual communication in elasmobranchs. In: Ladich F, Collin SP, Moller P, Kapoor BG, editors. Communication in fishes. Enfield (NH): Science Publishers, Inc. p. 337–392.

Hart NS, Lisney TJ, Marshall NJ, Collin SP. 2004. Multiple cone visual pigments and the potential for trichromatic colour vision in two species of elasmobranch. *J Exp Biol.* 207(26):4587–4594.

Hart NS, Theiss SM, Harahush BK, Collin SP. 2011. Microspectrophotometric evidence for cone monochromacy in sharks. *Naturwissenschaften* 98(3):193–201.

Heinicke MP, Naylor GJP, Hedges SB. 2009. Cartilaginous fishes (Chondrichthyes). In: Hedges SB, Kumar S, editors. The timetree of life. New York: Oxford University Press. p. 320–327.

Hoang DT, Chernomor O, von Haeseler A, Minh BQ, Vinh LS. 2018. UFBoot2: improving the ultrafast bootstrap approximation. *Mol Biol Evol.* 35(2):518–522.

Hope AJ, Partridge JC, Dulai KS, Hunt DM. 1997. Mechanisms of wavelength tuning in the rod opsins of deep-sea fishes. *Proc R Soc Lond B.* 264(1379):155–163.

Hunt DM, Dulai KS, Partridge JC, Cottrill P, Bowmaker JK. 2001. The molecular basis for spectral tuning of rod visual pigments in deep-sea fish. *J Exp Biol.* 204(Pt 19):3333–3344.

Hunt DM, Fitzgibbon J, Slobodyanyuk SJ, Bowmaker JK. 1996. Spectral tuning and molecular evolution of rod visual pigments in the species flock of cottoid fish in Lake Baikal. *Vision Res.* 36(9):1217–1224.

Imai H, Kojima D, Oura T, Tachibanaki S, Terakita A, Shichida Y. 1997. Single amino acid residue as a functional determinant of rod and cone visual pigments. *Proc Natl Acad Sci U S A.* 94(6):2322–2326.

Inoue JG, Miya M, Lam K, Tay B-H, Danks JA, Bell J, Walker TI, Venkatesh B. 2010. Evolutionary origin and phylogeny of the modern holocephalans (Chondrichthyes: Chimaeriformes): a mitogenomic perspective. *Mol Biol Evol.* 27(11):2576–2586.

Jacobs GH. 2009. Evolution of colour vision in mammals. *Philos Trans R Soc B.* 364(1531):2957–2967.

Jacobs GH, Deegan JF, Neitz J, Crognale MA, Neitz M. 1993. Photopigments and color vision in the nocturnal monkey, Aotus. *Vision Res.* 33(13):1773–1783.

Janz JM, Farrens DL. 2001. Engineering a functional blue-wavelength-shifted rhodopsin mutant. *Biochemistry* 40(24):7219–7227.

Janz JM, Farrens DL. 2004. Role of the retinal hydrogen bond network in rhodopsin Schiff base stability and hydrolysis. *J Biol Chem.* 279(53):55886–55894.

Jerlov NG. 1976. Marine optics. Amsterdam: Elsevier Scientific Publishing Company.

Joesch M, Meister M. 2016. A neuronal circuit for colour vision based on rod–cone opponency. *Nature* 532(7598):236–239.

Kalmijn AJ. 1971. The electric sense of sharks and rays. *J Exp Biol.* 55(2):371–383.

Katoh K, Standley DM. 2013. MAFFT multiple sequence alignment software version 7: improvements in performance and usability. *Mol Biol Evol.* 30(4):772–780.

Kelber A, Roth L. 2006. Nocturnal colour vision – not as rare as we might think. *J Exp Biol.* 209(5):781–788.

Kuwayama S, Imai H, Hirano T, Terakita A, Shichida Y. 2002. Conserved proline residue at position 189 in cone visual pigments as a determinant of molecular properties different from rhodopsins. *Biochemistry* 41(51):15245–15252.

Lamb TD, Hunt DM. 2017. Evolution of the vertebrate phototransduction cascade activation steps. *Dev Biol.* 431(1):77–92.

Lamb TD, Kraft TW. 2016. Quantitative modeling of the molecular steps underlying shut-off of rhodopsin activity in rod phototransduction. *Mol Vis.* 22:674–696.

Lamb TD, Patel H, Chuah A, Natoli RC, Davies WIL, Hart NS, Collin SP, Hunt DM. 2016. Evolution of vertebrate phototransduction: cascade activation. *Mol Biol Evol.* 33(8):2064–2087.

Levenson DH, Dizon A. 2003. Genetic evidence for the ancestral loss of short-wavelength-sensitive cone pigments in mysticete and odontocete cetaceans. *Proc R Soc Lond B.* 270(1516):673–679.

Lin SW, Kochendoerfer GG, Carroll KS, Wang D, Mathies RA, Sakmar TP. 1998. Mechanisms of spectral tuning in blue cone visual pigments.

Visible and raman spectroscopy of blue-shifted rhodopsin mutants. *J Biol Chem*. 273(38):24583–24591.

Lind O, Kelber A. 2011. The spatial tuning of achromatic and chromatic vision in budgerigars. *J Vis*. 11(7):2.

Loew ER, Lythgoe JN. 1978. The ecology of cone pigments in teleost fishes. *Vision Res*. 18(6):715–722.

Lythgoe JN. 1968. Visual pigments and visual range underwater. *Vision Res*. 8(8):997–1011.

Lythgoe JN, Muntz WRA, Partridge JC, Shand J, Williams DM. 1994. The ecology of the visual pigments of snappers (Lutjanidae) on the Great Barrier Reef. *J Comp Physiol A*. 174:461–467.

Meredith RW, Gatesy J, Emerling CA, York VM, Springer MS. 2013. Rod monochromacy and the coevolution of cetacean retinal opsins. *PLoS Genet*. 9(4):e1003432.

Munz FW, McFarland WN. 1973. The significance of spectral position in the rhodopsins of tropical marine fishes. *Vision Res*. 13(10):1829–1874.

Musilova Z, Cortesi F, Matschiner M, Davies WIL, Patel JS, Stieb SM, de Busserolles F, Malmstrøm M, Tørresen OK, Brown CJ, et al. 2019. Vision using multiple distinct rod opsins in deep-sea fishes. *Science* 364(6440):588–592.

Nathans J. 1990a. Determinants of visual pigment absorbance: identification of the retinylidene Schiff's base counterion in bovine rhodopsin. *Biochemistry* 29(41):9746–9752.

Nathans J. 1990b. Determinants of visual pigment absorbance: role of charged amino acids in the putative transmembrane segments. *Biochemistry* 29(4):937–942.

Naylor GJP, Caira JN, Jensen K, Rosana KAM, Straube N, Lakner C. 2012. Elasmobranch phylogeny: a mitochondrial estimate based on 595 species. In: Carrier JC, Musick JA, Heithaus MR, editors. Biology of sharks and their relatives. Boca Raton (FL): CRC Press. p. 31–56.

Neitz M, Neitz J, Jacobs GH. 1991. Spectral tuning of pigments underlying red-green color vision. *Science* 252(5008):971–974.

Newman LA, Robinson PR. 2005. Cone visual pigments of aquatic mammals. *Vis Neurosci*. 22(6):873–879.

Nguyen L-T, Schmidt HA, von Haeseler A, Minh BQ. 2015. IQ-TREE: a fast and effective stochastic algorithm for estimating maximum-likelihood phylogenies. *Mol Biol Evol*. 32(1):268–274.

Okano T, Fukada Y, Artamonov ID, Yoshizawa T. 1989. Purification of cone visual pigment from chicken retina. *Biochemistry* 28(22):8848–8856.

Okano T, Kojima D, Fukada Y, Shichida Y, Yoshizawa T. 1992. Primary structures of chicken cone visual pigments: vertebrate rhodopsins have evolved out of cone visual pigments. *Proc Natl Acad Sci U S A*. 89(13):5932–5936.

Paulsen R, Miller JA, Brodie AE, Bownds MD. 1975. The decay of long-lived photoproducts in the isolated bullfrog rod outer segment: relationship to other dark reactions. *Vision Res*. 15(12):1325–1332.

Peichl L. 2005. Diversity of mammalian photoreceptor properties: adaptations to habitat and lifestyle? *Anat Rec*. 287:1001–1012.

Peichl L, Behrmann G, Kröger R. 2001. For whales and seals the ocean is not blue: a visual pigment loss in marine mammals. *Eur J Neurosci*. 13(8):1520–1528.

Peirson SN, Halford S, Foster RG. 2009. The evolution of irradiance detection: melanopsin and the non-visual opsins. *Philos Trans R Soc B*. 364(1531):2849–2865.

Pisani D, Mohun SM, Harris SR, McInerney JO, Wilkinson M. 2006. Molecular evidence for dim-light vision in the last common ancestor of the vertebrates. *Curr Biol*. 16(9):R318–R319.

Priyam A, Woodcroft BJ, Rai V, Munagala A, Moghul I, Ter F, Chowdhary H, Pieniak I, Maynard LJ, Gibbins MA, et al. 2019. Sequenceserver: a modern graphical user interface for custom BLAST databases. *Mol Biol Evol*. msz185, https://doi.org/10.1093/molbev/msz185.

Reitner A, Sharpe LT, Zrenner E. 1991. Is colour vision possible with only rods and blue-sensitive cones? *Nature* 352(6338):798–800.

Renz AJ, Meyer A, Kuraku S. 2013. Revealing less derived nature of cartilaginous fish genomes with their evolutionary time scale inferred with nuclear genes. *PLoS One* 8(6):e66400.

Ripps H, Dowling JE. 1990. Structural features and adaptive properties of photoreceptors in the skate retina. *J Exp Zool*. 256(S5):46–54.

Roorda A, Metha AB, Lennie P, Williams DR. 2001. Packing arrangement of the three cone classes in primate retina. *Vision Res*. 41(10–11):1291–1306.

Sabbah S, Hawryshyn CW. 2013. What has driven the evolution of multiple cone classes in visual systems: object contrast enhancement or light flicker elimination? *BMC Biol*. 11(1):77.

Sato K, Yamashita T, Kojima K, Sakai K, Matsutani Y, Yanagawa M, Yamano Y, Wada A, Iwabe N, Ohuchi H, et al. 2018. Pinopsin evolved as the ancestral dim-light visual opsin in vertebrates. *Commun Biol*. 1:156.

Schieber NL, Collin SP, Hart NS. 2012. Comparative retinal anatomy in four species of elasmobranch. *J Morphol*. 273(4):423–440.

Schluessel V, Rick IP, Plischke K. 2014. No rainbow for grey bamboo sharks: evidence for the absence of colour vision in sharks from behavioural discrimination experiments. *J Comp Physiol A*. 200(11):939–947.

Scholtyssek C, Kelber A, Dehnhardt G. 2015. Why do seals have cones? Behavioural evidence for colour-blindness in harbour seals. *Anim Cogn*. 18(2):551–560.

Sorenson L, Santini F, Alfaro ME. 2014. The effect of habitat on modern shark diversification. *J Evol Biol*. 27(8):1536–1548.

Stell WK. 1972. The structure and morphologic relations of rods and cones in the retina of the spiny dogfish, *Squalus*. *Comp Biochem Phys A*. 42(1):141–151.

Szamier RB, Ripps H. 1983. The visual cells of the skate retina: structure, histochemistry, and disc-shedding properties. *J Comp Neurol*. 215(1):51–62.

Takahashi Y, Ebrey TG. 2003. Molecular basis of spectral tuning in the newt short wavelength sensitive visual pigment. *Biochemistry* 42(20):6025–6034.

Takenaka N, Yokoyama S. 2007. Mechanisms of spectral tuning in the RH2 pigments of Tokay gecko and American chameleon. *Gene* 399(1):26–32.

Theiss SM, Davies WI, Collin SP, Hunt DM, Hart NS. 2012. Cone monochromacy and visual pigment spectral tuning in wobbegong sharks. *Biol Lett*. 8(6):1019–1022.

Theiss SM, Lisney TJ, Collin SP, Hart NS. 2007. Colour vision and visual ecology of the blue-spotted maskray, *Dasyatis kuhlii* Muller & Henle, 1814. *J Comp Physiol A*. 193:67–79.

Van-Eyk SM, Siebeck UE, Champ CM, Marshall J, Hart NS. 2011. Behavioural evidence for colour vision in an elasmobranch. *J Exp Biol*. 214(24):4186–4192.

Vélez-Zuazo X, Agnarsson I. 2011. Shark tales: a molecular species-level phylogeny of sharks (Selachimorpha, Chondrichthyes). *Mol Phylogenet Evol*. 58(2):207–217.

Vorobyev M. 1997. Costs and benefits of increasing the dimensionality of colour vision system. In: Taddei-Ferretti C, editor. Biophysics of photoreception: molecular and phototransductive events. Singapore: World Scientific. p. 280–289.

Wakefield MJ, Anderson M, Chang E, Wei KJ, Kaul R, Graves JA, Grutzner F, Deeb SS. 2008. Cone visual pigments of monotremes: filling the phylogenetic gap. *Vis Neurosci*. 25(3):257–264.

Walls GL. 1963. The vertebrate eye and its adaptive radiation. New York/London: Hafner Publishing Company.

Yanagawa M, Kojima K, Yamashita T, Imamoto Y, Matsuyama T, Nakanishi K, Yamano Y, Wada A, Sako Y, Shichida Y. 2015. Origin of the low thermal isomerization rate of rhodopsin chromophore. *Sci Rep*. 5:11081.

Yokoyama S. 2008. Evolution of dim-light and color vision pigments. *Annu Rev Genom Hum Genet*. 9(1):259–282.

Yokoyama S. 2000. Molecular evolution of vertebrate visual pigments. *Prog Retin Eye Res*. 19(4):385–419.

Yokoyama S, Radlwimmer FB. 2001. The molecular genetics and evolution of red and green color vision in vertebrates. *Genetics* 158(4):1697–1710.

Yokoyama S, Takenaka N, Blow N. 2007. A novel spectral tuning in the short wavelength-sensitive (SWS1 and SWS2) pigments of bluefin killifish (*Lucania goodei*). *Gene* 396(1):196–202.

Yokoyama S, Yang H, Starmer WT. 2008. Molecular basis of spectral tuning in the red- and green-sensitive (M/LWS) pigments in vertebrates. *Genetics* 179(4):2037–2043.

Yokoyama S, Zhang H, Radlwimmer FB, Blow NS. 1999. Adaptive evolution of color vision of the Comoran coelacanth (*Latimeria chalumnae*). *Proc Natl Acad Sci U S A.* 96(11):6279–6284.

Zhang X, Wensel TG, Yuan C. 2006. Tokay gecko photoreceptors achieve rod-like physiology with cone-like proteins. *Photochem Photobiol.* 82:1452–1460.